Selective catalytic reduction of NO_x with ammonia and hydrocarbon oxidation over V_2O_5-MoO_3/TiO_2 and V_2O_5-WO_3/TiO_2 SCR catalysts

Lei Zheng[1], Maria Casapu[1], Matthias Stehle[1], Olaf Deutschmann[1], Jan-Dierk Grunwaldt[1,*]

[1]Institute for Chemical Technology and Polymer Chemistry (ITCP), Karlsruhe Institute of Technology (KIT), Engesserstraße 20, 76131 Karlsruhe, Germany

*Corresponding author: grunwaldt@kit.edu (J.-D. Grunwaldt)

Abstract

The NH_3-SCR performance in the presence of short and long chain hydrocarbons (propylene and dodecane) as well as of formaldehyde was investigated for a series of V_2O_5-MoO_3/TiO_2 (VMoTi) and V_2O_5-WO_3/TiO_2 (VWTi) catalysts. The results demonstrate that vanadium oxides act as the main catalytically active component for NO_x conversion, hydrocarbon (HC) and formaldehyde oxidation. Among VMoTi and VWTi materials with different vanadium loading, the catalysts containing 3 wt.% V_2O_5 lead to the highest catalytic activity. The ability to simultaneously remove NO_x, HC and HCHO over VMoTi is inferior to that of the conventional WO_3-based catalyst. However, VMoTi exhibits higher CO_2 selectivity, especially during oxidation of long-chain HCs, which represents an important advantage for a possible multifunctional catalyst. Apart from CO, formaldehyde was detected as byproduct during HC oxidation for both catalyst formulations.

Keywords: SCR, DPF, hydrocarbon oxidation, formaldehyde, vanadium, molybdenum

1. Introduction

Selective catalytic reduction (SCR) of NO_x with ammonia is to date the best-developed and most widespread method for NO_x removal [1-3]. SCR catalysts based on vanadia and metal exchanged zeolites are proven technologies for NO_x reduction in diesel engines. Cu- or Fe-exchanged zeolites are particularly used for low temperature applications [4,5]. Vanadia-catalysts are widely applied for NO_x reduction in heavy-duty diesel engines, for natural gas engines and other stationary applications due to their good NO_x conversion efficiency and high durability against sulfur-poisoning [6-8]. Particularly the last aspect is highly important for NO_x removal systems in emerging countries, where the sulfur content in fuel is still significant (in some regions >50 ppm, [9]). Commercial vanadia-based SCR catalysts typically contain titania as support, vanadia as active component and tungsten or molybdenum oxide as structural and chemical promoters, i.e. V_2O_5-WO_3/TiO_2 and V_2O_5-MoO_3/TiO_2 (VWT and VMoTi, respectively) [3]. The anatase TiO_2 with high surface area possesses high acidity and high resistance against sulfur poisoning [10] whereas the well dispersed vanadium species, below a monolayer coverage, have been reported as the redox active component in NO_x reduction [11,12]. Both WO_3 and MoO_3 promoters improve the SCR performance of the binary V_2O_5/TiO_2 catalyst, with the first one being more active but also less resistant to As poisoning, that is present in flue gases [13]. In addition, both catalyst formulations show potential for hydrocarbon (HC) and soot oxidation [14], which makes them promising candidates for SCR on diesel particulate filter applications (SCR-DPF) if the temperature can be kept below 550 °C [15-17]. Such

a combination allows a faster warm-up due to the closer location to the engine. Consequently, this may also lead to higher NO_x conversion during the cold start phase of the engine. Moreover, it could significantly reduce the costs and the overall volume of the exhaust aftertreatment system. Finally, the recently reported ability to lower formaldehyde emissions in the exhaust of natural gas engines [18], increases the relevance of such catalyst formulations.

Hydrocarbons are particularly emitted during the cold start period when the temperature of the exhaust gas stream is not high enough and even during the warm-up period upon the deactivation of the diesel oxidation catalysts (DOC) [19,20]. The composition of such emissions highly depends on various factors like fuel properties, engine characteristics or engine operation conditions. For natural gas engines, in addition to methane emissions, formaldehyde is typically generated by partial oxidation of methane [21], and requires a special consideration due to its toxicity. Several recent studies report the ability of V-W-based SCR catalysts to oxidize different classes of volatile organic compounds (VOCs) simultaneously to their NO_x-removal activity [22-24,18]. The oxidation activity of V_2O_5-based catalysts for carbonaceous species has been linked to the low oxygen bond strength of vanadia [25]. Watling et al. [26] showed that up to 80% of propylene conversion is achieved at 550 °C on commercial vanadia based SCR catalysts, without a significant impact on the SCR performance. A similarly high SCR activity was observed by Bertole et al. [18] in the presence of HCHO, CO, C_2H_4 and C_2H_6 over a V-based system that also included noble metals. Ottinger et al. [27] investigated the capability of vanadia-based catalysts for oxidizing long-chain HCs such as dodecane. They observed a poor selectivity towards CO_2 formation. In addition, they also found that certain HCs could lead to deactivation of vanadia-based catalysts due to adsorption and accumulation on the surface and thus blocking of the active sites. Heo et al. [28] showed that the presence of propylene leads to lower NO_x conversion due to the competition between ammonia and propylene during adsorption and also to the promotion of ammonia oxidation at higher temperatures. In a previous study, the promising ability of vanadia-based SCR catalysts for hydrocarbon and soot oxidation has been reported [29], which is strongly limited by the low CO_2 selectivity.

In addition to V_2O_5, MoO_3 is also well known for its ability to oxidize VOCs and soot [30-36]. In fact, when comparing alumina supported V_2O_5 and MoO_3 catalysts, a lower temperature for soot oxidation and a higher CO_2 selectivity was recorded for the molybdenum-based sample [30]. In contrast, V_2O_5/TiO_2 was found to be more active for methanol and n-butyl acetate oxidation in comparison with MoO_3/TiO_2 [35]. Furthermore, a strong synergistic effect was observed between MoO_3 and V_2O_5 supported on TiO_2 during total oxidation of benzene and chlorobenzene, similar as that present in WO_3-V_2O_5/TiO_2 catalysts [31,36]. In this context, investigation of the NO_x and HC removal activity of catalysts containing both, V_2O_5 and MoO_3, is highly interesting. Hence, in the present study the NH_3-SCR performance in the presence of HCs and HCHO has been systematically evaluated for a series of VMoTi catalysts, containing different V_2O_5 loadings, and compared to that of WTi-based catalysts.

2. Materials and Methods

VMoTi and VWTi catalysts were synthesized by incipient wetness impregnation of titania (Alfa Aesar, structural properties, cf. Table 1). Ammonium metavanadate (Sigma Aldrich), ammonium metatungstate hydrate (Fluka) and ammonium heptamolybdat (Merck) were used as precursors for V_2O_5, WO_3 and MoO_3, respectively. Several samples were prepared by varying the V_2O_5 loading, i.e. 1, 3 and 5 wt.% on the 9 wt.% WO_3-TiO_2 or 9 wt.% MoO_3-TiO_2

supports. A detailed description of procedures is available in the Supplementary Information (SI). In the following the samples will be referred to as e.g. 1V-WTi and 1V-MoTi for the 1 wt.% V_2O_5 loaded catalysts, 3V-WTi and 3V-MoTi for the 3 wt.% V_2O_5 loaded catalysts and so on.

All samples were characterized by N_2 physisorption, X-ray diffraction (XRD), UV-vis spectroscopy, Raman spectroscopy and temperature-programmed desorption of ammonia (NH_3-TPD). A detailed description of the procedures is available in the SI.

The catalytic tests were carried out under steady-state conditions using a quartz tube plug flow reactor, as described in detailed in the SI. The gas concentrations were 500 ppm NO, 500 ppm NH_3, 5% H_2O, 10% O_2 in N_2 (standard SCR) with 185 ppm C_3H_6, 80 ppm $C_{12}H_{26}$ or 50 ppm HCHO dosed optionally (50000 h^{-1}). HC oxidation tests were performed using 185 ppm C_3H_6 (or 80 ppm $C_{12}H_{26}$, or 50 ppm HCHO), 5% H_2O and 10% O_2 in N_2 (50000 h^{-1}). The gas composition was analyzed with a MultiGas^{TM} 2030 FTIR gas analyzer (MKS). During the catalytic activity tests the fluctuations of the FTIR derived gas concentrations were about ±1-2 ppm.

3. Results

3.1 Characterization

The surface area (S_{BET}), the pore volume (V_p), the mean pore diameter (d_p) and the V_2O_5, WO_3 and MoO_3 coverage (θ_V, θ_W and θ_{Mo}, respectively) of the investigated samples are reported in Table 1. The surface area of the TiO_2 support was 101 m^2/g and decreased to 88 m^2/g after impregnation with 9 wt.% WO_3 or MoO_3. Further impregnation of V_2O_5 led to a significant decrease of the surface area, particularly for higher V loadings. A more pronounced decrease was found for VMoTi catalysts. For example, a surface area of only 68 m^2/g was measured for 3V-MoTi as compared to 82 m^2/g for 3V-WTi. This is in accordance with previous studies reporting that Mo-promoted catalysts exhibit lower surface area compared to the catalysts containing WO_3 [13,37].

Table 1. Structure and morphological characterization of the investigated samples.

Sample	S_{BET} (m^2/g)	V_p (mL/g)	d_p (nm)	θ_V	θ_W	θ_{Mo}	Total number of acidic sites [a]
TiO_2	101	0.37	14.86	-	-	-	-
3V-Ti	65	0.34	20.69	0.19	-	-	-
W-Ti	88	0.32	14.41	-	0.63	-	-
Mo-Ti	88	0.31	14.01	-	-	0.93	-
1V-WTi	83	0.32	15.24	0.05	0.67	-	1.05
3V-WTi	82	0.32	15.67	0.15	0.68	-	1.00
5V-WTi	52	0.28	21.64	0.40	1.07	-	0.49
1V-MoTi	86	0.33	15.47	0.05	-	0.95	0.84
3V-MoTi	68	0.29	17.05	0.18	-	1.20	0.67
5V-MoTi	37	0.20	21.80	0.57	-	2.21	0.39

[a] relative total number of acidic sites normalized by 3V-WTi.

The metal oxide coverage was calculated based on a monolayer capacity of 0.145 wt.% V_2O_5/m^2 [38], 7 µmol/m^2 for WO_3 [39] and 0.12 wt.% MoO_3/m^2 [13]. As shown in Table 1, it appears that the theoretical monolayer coverage in

terms of (WO_3+ V_2O_5) is achieved for the 3V-WTi sample and is exceeded for the 5V-WTi catalyst. In contrast, for the Mo-containing series the monolayer coverage is reached already for 1 wt.% loading of V. According to previous studies, a monolayer coverage of V species leads to the highest SCR performance [11] whereas vanadia-agglomerates appearing for higher loadings enhance the parasitic ammonia oxidation at high temperatures [40].

Temperature programmed desorption of ammonia (NH_3-TPD) was carried out to investigate the acidic properties of the catalyst surface (Fig. 1). Assuming the typical Eley-Rideal mechanism, ammonia participates in the SCR reaction from an adsorbed state and the activity is closely correlated with the acidity of the catalysts [3,41]. The temperature range of 125-350 °C is assigned to relatively weak acidic sites, which are the most relevant for the SCR performance [42]. Fig. 1 shows that the majority of acidic sites emerge in the temperature range from 150-300 °C for both series of catalysts. A slightly higher acidity was measured for VWTi catalysts over the corresponding VMoTi catalysts (total acidic sites normalized by 3V-WTi are reported in Table 1). However, the major difference was observed in the amount of strong acidic sites. NH_3 adsorbed at these sites desorbs above 350 °C and seems to be almost inexistent for the Mo-based catalysts. NH_3 desorption at such elevated temperatures was previously associated with Brønsted acidic sites, according to in-situ DRIFTS experiments reported by Song et al. [43].

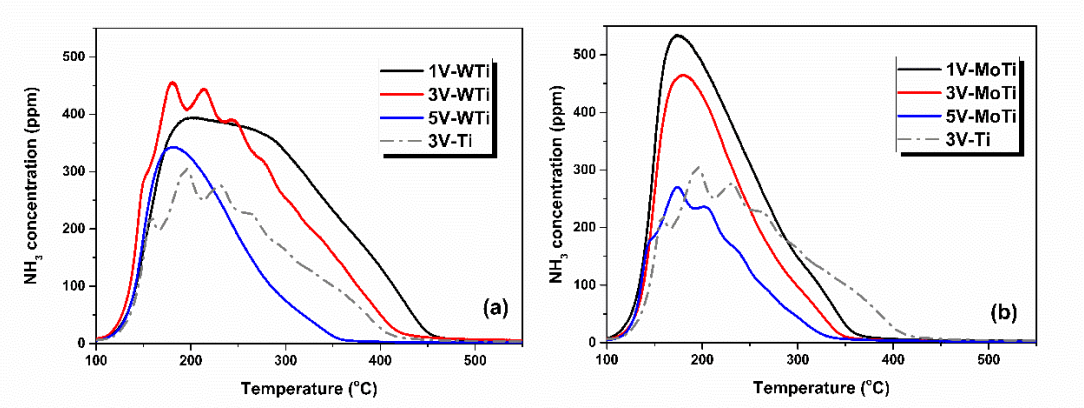

Figure 1. NH_3-TPD results for (a) VWTi and (b) VMoTi catalysts.

The Raman spectra of the titania support, VWTi and VMoTi catalysts are depicted in Fig. 2 and mainly contain bands at 145, 197, 397, 528 and 637 cm^{-1}. They are attributed to the anatase phase [44,45]. In the range between 800 cm^{-1} and 1200 cm^{-1} (Fig. 2b), the band at 969 cm^{-1} that appears for WTi was previously assigned to the symmetric stetching vibration of the W=O bond [46]. The presence of polymeric vanadates in all V-W catalysts is indicated by the bands at 976, 987 and 989 cm^{-1} (V=O stretching vibrations [47]). With increasing V_2O_5 loading, the V=O stretching band shifted to higher wavenumbers, most probably due to the polymerization of the vanadyl species [47]. Nevertheless, the shoulder at 1020 cm^{-1} from 5V-WTi sample originates from V=O stretching and indicates the presence of isolated vanadyls [48,47,5].

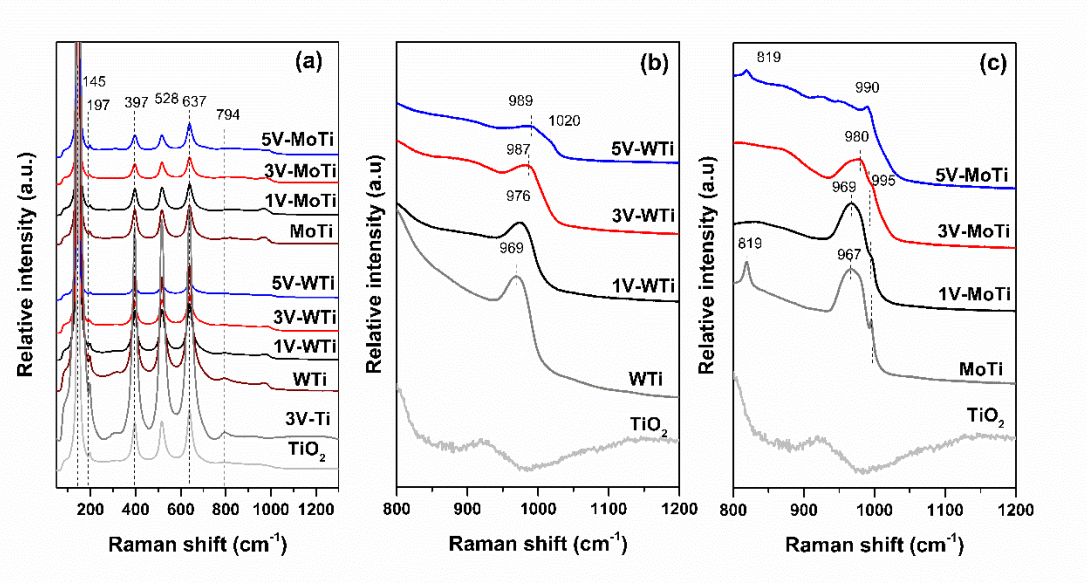

Figure 2. Raman spectra of investigated samples: (a) VWTi and VMoTi (50-1300 cm^{-1}), (b) VWTi (800-1200 cm^{-1}) and (c) VMoTi (800-1200 cm^{-1}).

Raman spectra of VMoTi catalysts in the range of 800-1200 cm^{-1} are shown in Fig. 2(c). The band at 967 cm^{-1} observed for MoTi was previously related to the Mo-O bending and stretching modes [49]. The bands at 819 and 955 cm^{-1} were attributed to crystalline and isolated MoO_3 species, respectively [49]. The band at 995 cm^{-1} decreased progressly with V_2O_5 loading, which is attributeded to surface disorder of nanoparticles [47,50]. Furthermore, no isolated MoO_3 species were observed for 5V-MoTi. In contrast, a new peak at 819 cm^{-1} corresponding to crystalline MoO_3 species appeared for 5V-MoTi. This indicates that with increasing of V_2O_5 loading the Mo phase transformed progressively from isolated to crystalline MoO_3 species. Furthermore, 1V-MoTi, 3V-MoTi and 5V-MoTi samples show bands at 969, 980 and 990 cm^{-1} respectively, which were attributed to the V=O stretching vibrations in polymeric vanadates. Similarly as for VWTi catalysts, stronger polymerization of V-species was also found with increasing of V_2O_5 loading [47].

According to the XRD and UV-vis results, a higher V_2O_5 content leads also to the formation of progressively larger TiO_2 crystallites (XRD, Fig. S1), which is probably the origin of the more pronounced absorption in the 400-800 nm region (UV-vis, Fig. S2).

3.2 Hydrocarbon oxidation on VMoTi and VWTi catalysts

3.2.1 Propylene oxidation

The 3wt.% V samples showed the best activity for C_3H_6 oxidation, with full conversion observed at 350 °C and 400 °C for W and Mo promoted catalysts, respectively (Fig. 3). At 200 °C the W- and Mo-catalysts oxidized about 30% and 15% C_3H_6, respectively (Fig. 3). The superior oxidation performance at low temperatures of 3V-WTi in comparison to 3V-MoTi is analogous to the NO_x removal activity of the two catalysts under standard SCR conditions (Fig. S3). The 3V-WTi samples converted about 95% NO_x at 200 °C whereas only 68% conversion was observed for 3V-MoTi

(Fig. S3). Regarding the V content, the samples with a vanadia loading of 3% exhibited the highest NO_x removal and propylene oxidation activity (further details in Fig. S3 and S4), followed by the samples with 5% and 1% vanadia content. The corresponding CO, CO_2 and formaldehyde emissions of propylene oxidation over the 3V-WTi and 3V-MoTi are shown in Fig. 3 (b). The partial oxidation of HCs over vanadia-based catalysts leads to a mixture of CO and CO_2 instead of total oxidation, which has been previously reported also for commercial catalysts [26,29]. Accordingly, in the present study, the CO share was much higher than the CO_2 concentration for both catalysts, which is in agreement with our previous results [29]. The slight decrease of the CO_2 and CO concentration around 500 °C while formaldehyde was still fully converted suggest the possible formation of additional oxidation products, which could not be identified in the present study. The formaldehyde emissions reached a maximum of only 8.5 ppm for 3V-WTi at 300 °C but of 22.3 ppm for 3V-MoTi at 350 °C, at temperatures above 450 °C no formaldehyde formation was recorded in both cases. Such emissions at lower temperatures were reported also in a recent study of Bertole et al. [18] on propane and propylene oxidation over V-based catalysts. Fig. 3 (c) shows the corresponding $[CO_2]/([CO]+[CO_2])$ ratios obtained at 200, 300 and 400 °C during C_3H_6 oxidation. Obviously, there is no clear trend when comparing the two catalysts. At 400 °C the same ratio was obtained for both catalysts. At 300 °C the 3V-WTi sample showed about 10% higher selectivity towards CO_2 formation whereas at 200 °C an almost opposite situation was recorded.

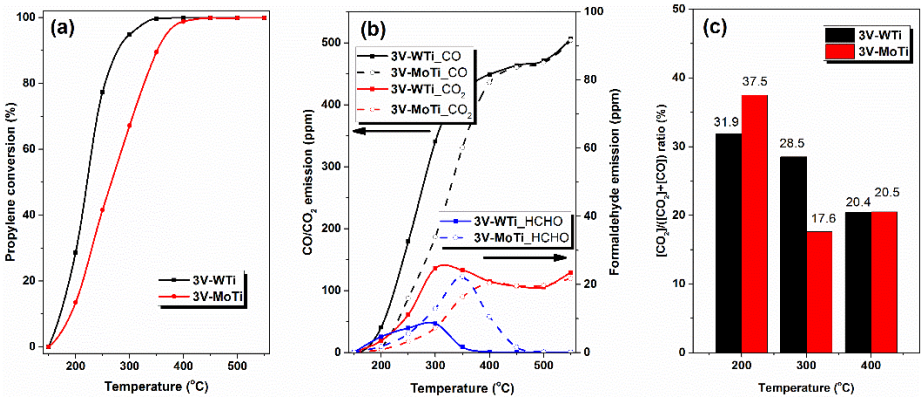

Figure 3. Propylene oxidation over 3V-WTi and 3V-MoTi catalysts: (a) propylene conversion; (b) CO, CO_2 and formaldehyde emission; (c) $[CO_2]/([CO]+[CO_2])$ ratio at 200, 300 and 400 °C. C_3H_6: 185 ppm, O_2: 10%, H_2O: 5%, N_2 for balance, GHSV=50 000 h^{-1}.

3.2.2 Dodecane oxidation

Considering the superior C_3H_6 oxidation performance of the 3 wt.% vanadia catalysts among the differently loaded samples, dodecane and formaldehyde oxidation as well as SCR activity in the presence of HCs were only evaluated for the 3V-WTi and 3V-MoTi catalysts. Dodecane oxidation activity obtained for 3V-WTi and 3V-MoTi is shown in Fig. 4. For both catalysts, full conversion was achieved above 300 °C. Also in this case, the W-containing sample showed a higher activity at lower temperatures. This amounted to about 81% dodecane conversion at 150 °C, in comparison to only 52% obtained over 3V-MoTi. Formation of CO is higher than that of CO_2 above 300 °C for both catalysts. The selectivity towards CO_2 formation was slightly higher for the molybdenum sample (Fig. 4b). At 200 °C

the $[CO_2]/([CO]+[CO_2])$ ratio over 3V-WTi was about 65% whereas for the Mo-catalyst it amounted to ~76%. HCHO emissions of about 7 ppm were measured for both catalysts, appearing especially at lower temperatures.

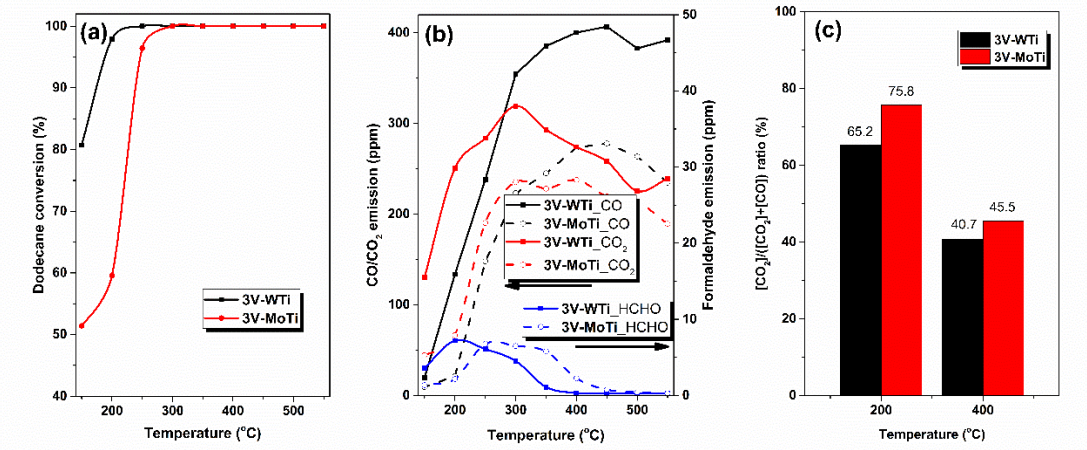

Figure 4. Dodecane oxidation over 3V-WTi and 3V-MoTi catalysts: (a) dodecane conversion; (b) CO, CO_2 and formaldehyde emission; (c) $[CO_2]/([CO]+[CO_2])$ ratio at 200 and 400 °C. $C_{12}H_{26}$: 80 ppm, O_2: 10%, H_2O: 5%, N_2 for balance, GHSV=50 000 h^{-1}.

3.2.3 Formaldehyde oxidation

The appearance of formaldehyde emissions during propylene and dodecane oxidation, especially at low temperatures, has been further tackled by measuring the HCHO oxidation activity for the 3V-WTi and 3V-MoTi catalysts (Fig. 5). Full conversion was only observed above 300 °C or 400 °C for W- and Mo-samples, respectively. Similarly to the propylene and dodecane oxidation, at lower temperatures the W-containing catalyst showed a higher activity. In contrast to the oxidation of propylene and dodecane, which led to relatively high $[CO_2]/([CO]+[CO_2])$ ratios, the CO emissions were dominant during formaldehyde conversion (Fig. 5 (c)).

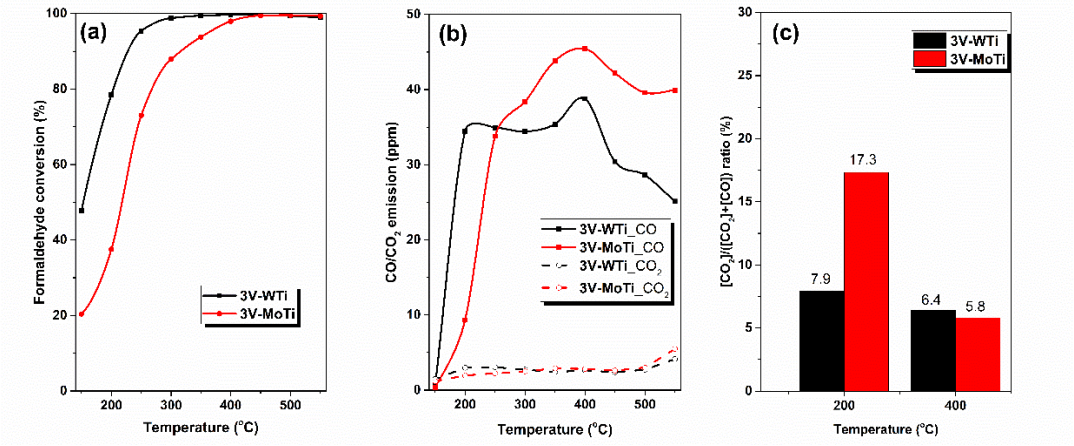

Figure 5. Formaldehyde oxidation over 3V-WTi and 3V-MoTi catalysts: (a) formaldehyde conversion; (b) CO and CO_2 emission; (c) $[CO_2]/([CO]+[CO_2])$ ratio. HCHO: 50 ppm, O_2: 10%, H_2O: 5%, N_2 for balance, GHSV=50 000 h^{-1}

At high temperatures almost similar ratios were obtained whereas at 200 °C the 3V-MoTi sample shows about 10% higher $[CO_2]/([CO]+[CO_2])$ ratio. Above 400°C, the observed decrease of the CO concentration was not balanced by the slight increase of the CO_2 amount, suggesting a change of the oxidation mechanism and probably the formation of further oxidation products.

3.3 Standard SCR activity in the presence of hydrocarbons and formaldehyde

3.3.1 SCR with propylene oxidation

The presence of propylene did not significantly affect the NO_x conversion during SCR over both catalysts, as shown in Figs. 6 a and b. Only a slight decrease of about 3% was noticed at higher temperatures once the conversion of C_3H_6 started. This indicates that a competition for the active sites exists, which could lead to more pronounced effects for higher C_3H_6 concentrations in comparison to the one used in this study. Vice versa, at low temperatures C_3H_6 oxidation activity decreased under SCR conditions, probably due to the stronger NH_3 adsorption on the catalyst surface. This behavior is even more pronounced for the Mo-based catalyst, which shows a 100 °C shift for the onset of propylene oxidation. Hardly any inhibition of SCR on C_3H_6 oxidation was found above 400 °C for both catalysts, in agreement with previous literature studies [26,29]. Also in the presence of the SCR gas mixture formaldehyde emissions were recorded for both samples. However, a significantly lower HCHO concentration was observed over 3V-WTi under these reaction conditions (Fig. 6c). Regarding the $[CO_2]/([CO]+[CO_2])$ ratio resulting from propylene oxidation, slightly higher CO_2 concentrations were detected for both catalysts. This could be explained by the promoting effect of the more oxidative atmosphere under SCR condition, i.e. the presence of NO_x.

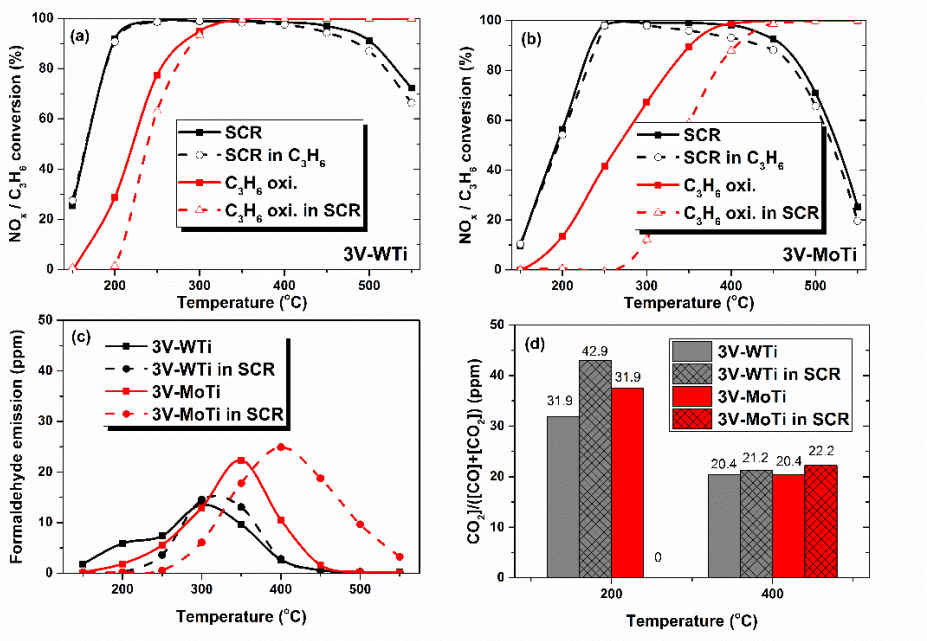

Figure 6. Standard SCR in presence of propylene over (a) 3V-WTi and (b) 3V-MoTi catalysts; (c) formaldehyde emission; (d) $[CO_2]/([CO]+[CO_2])$ ratio at 200 and 400 °C. C_3H_6: 185 ppm, NO: 500 ppm, NH_3: 500 ppm, O_2: 10%, H_2O: 5%, N_2 for balance, GHSV=50 000 h^{-1}.

3.3.2 SCR with dodecane oxidation

In contrast to the low effect induced by C_3H_6, dodecane inhibited the standard SCR activity of 3V-MoTi over the whole temperature range while the 3V-WTi catalyst maintained its activity between 250 °C and 450 °C, as shown in Fig. 7 (a). At 200 °C a drop in activity of more than 40% was found for 3V-MoTi and of over 50% for the W-containing catalyst. At higher temperatures, the deactivation extent decreased considerably for both sample. Fig. 7 (b) reports the dodecane oxidation performance with and without the standard SCR gas mixture. Full conversion of dodecane was obtained only above 250 °C for 3V-WTi and above 300 °C for 3V-MoTi. Analogous to propylene oxidation in the presence of the SCR gas mixture, this may be traced back to the competition for active sites. At the same time, the presence of standard SCR reduced the formaldehyde emissions for both catalysts at low temperatures. Furthermore, as shown in Fig. 7 (d), the standard SCR gas mixture promoted the CO_2 formation in both mid and high temperature range over both catalysts, with a higher $[CO_2]/([CO]+[CO_2])$ ratio for 3V-MoTi catalyst.

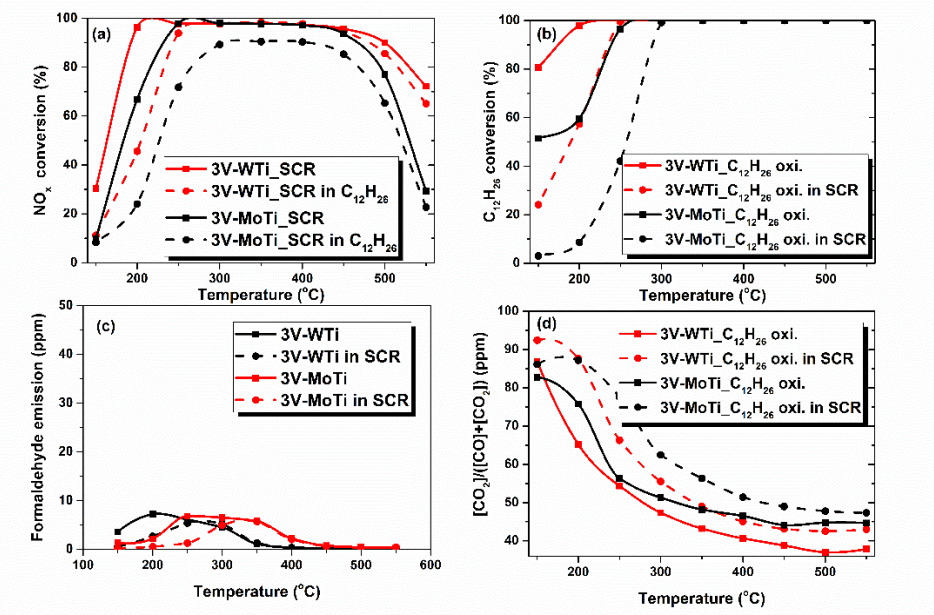

Figure 7. Standard SCR in presence of dodecane oxidation over 3V-WTi and 3V-MoTi: (a) standard SCR and (b) dodecane oxidation performance; (c) formaldehyde emission and (d) $[CO_2]/([CO]+[CO_2])$ ratio. $C_{12}H_{26}$: 80 ppm, NO: 500 ppm, NH_3: 500 ppm, O_2: 10%, H_2O: 5%, N_2 for balance, GHSV=50 000 h^{-1}.

3.3.3 SCR with formaldehyde oxidation

Fig. 8 (a) reports the standard SCR performance with and without the presence of the formaldehyde. It is observed that formaldehyde inhibits the standard SCR activity of 3V-MoTi over the whole temperature range while 3V-WTi catalyst maintained its $DeNO_x$ conversion above 350 °C. At 200 °C a drop in activity of 8% was measured for both W- and Mo-containing catalysts. At higher temperatures, the deactivation extent decreased gradually for both samples.

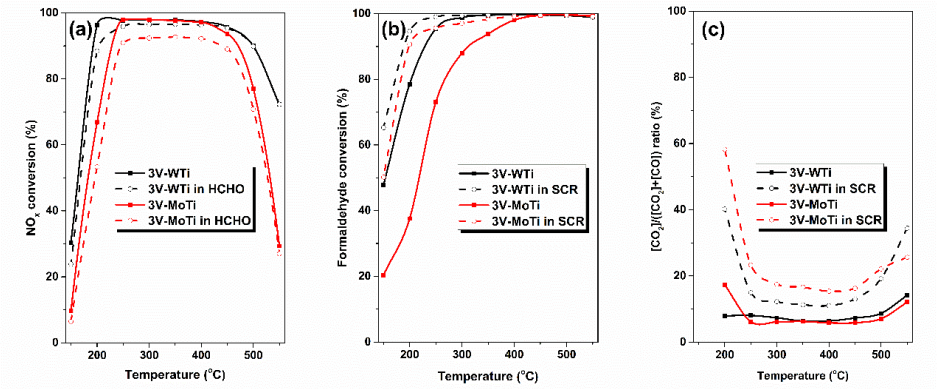

Figure 8. Standard SCR in presence of formaldehyde oxidation over 3V-WTi and 3V-MoTi: (a) standard SCR; (b) dodecane oxidation performance; (c) $[CO_2]/([CO]+[CO_2])$ ratio. HCHO: 50 ppm, NO: 500 ppm, NH_3: 500 ppm, O_2: 10%, H_2O: 5%, N_2 for balance, GHSV=50 000 h^{-1}.

In contrast to the inhibition effect of the standard SCR conditions on propylene and dodecane oxidation, increased formaldehyde conversion was observed over both catalysts in the low temperature range. At 200 °C an increase in activity of 16% was detected for 3V-WTi and of over 53% for the Mo-containing catalyst. Considering that both catalysts show high conversion, it appears that formaldehyde conversion is mainly influenced by the gas mixture and does not occur on the surface of Mo or W species. Similar to the oxidation of propylene and dodecane, during formaldehyde oxidation the standard SCR gas mixture promoted the CO_2 formation over both catalysts, with a higher $[CO_2]/([CO]+[CO_2])$ ratio observed for 3V-MoTi catalyst.

4. Discussion and conclusions

VWTi catalysts exhibit a broader temperature window for SCR and higher activity towards HC oxidation in comparison to the corresponding VMoTi catalysts. The difference could be explained by the higher surface area and higher surface acidity of W-containing catalysts. Especially the first assumption is supported by the almost identical NO_x removal performance of the 1 wt.%V_2O_5 samples (Fig. S3), which is in line with the results reported in literature for similar samples [13,37]. As indicated by XRD and Raman spectroscopy data (Fig. S1 and Fig. 2), higher vanadia loadings lead to sintering of the TiO_2 support and Mo-species [11]. Nevertheless, the 3 wt.% vanadia samples showed the highest SCR performance irrespective of the W or Mo presence as promoters.

Analogous to the standard SCR performance, the 3V-WTi and 3V-MoTi catalysts showed the highest C_3H_6 conversion, indicating that also in this case V sites are the main active species. This is supported by the already well-known activity of vanadia-catalysts for hydrocarbon oxidation [51], that is promoted by a low oxygen bond strength [25]. In spite of the reported similar or even superior soot oxidation activity of MoO_3 [30], its contribution to propylene oxidation is visible only at high temperatures for the vanadia-free samples (Fig. S4).

In contrast to C_3H_6 oxidation, $C_{12}H_{26}$ conversion occurs at much lower temperatures in the absence of the SCR mixture. This is a result of chain length impact since HCs with longer chain length are easier oxidized [25, 26]. This explains the substantial impact of dodecane presence on SCR activity, observed for both catalysts. The clear competition

between adsorption and activation of the SCR species and dodecane is reflected in the major decrease in activity at temperatures below 300 °C. According to the SCR reaction mechanism suggested by Topsøe et al. [52], NH_3 is first adsorbed on V-OH acid sites and then reacts with gas phase or weekly adsorbed NO, followed by reoxidation of V^{4+} sites in presence of O_2 (standard SCR) [53]. HCs compete with NH_3 for active V sites since both processes require the V-species for adsorption and activation [29]. In addition, CO and other intermediates can impede the reoxidation of V^{4+} sites, also inhibiting further conversion.

For both catalyst series, only a partial oxidation of hydrocarbons was recorded, resulting in high CO emissions, in accordance to previous studies [22-24, 27-29]. Slightly lower CO concentrations were measured in the presence of the standard SCR gas mixture, most probably due to the promoting effect of NO_x [54]. An increase of the $[CO_2]/([CO]+[CO_2])$ ratio of up to 23% was observed for the Mo-promoted samples in the presence or absence of the SCR mixture. Formaldehyde formation was uncovered during the propylene or dodecane oxidation tests. Although a higher concentration was recorded for 3V-MoTi in the absence of the SCR feed, the HCHO emissions reached the same level for the Mo- and W-based samples if NH_3 and NO were simultaneously dosed over the catalyst bed.

Regarding the formaldehyde oxidation ability as well as its interference with the standard SCR reactions, which is highly relevant for the exhaust aftertreatment system of natural gas engines, significant promotion of the SCR feed with respect to formaldehyde conversion was recorded at low temperatures for both 3 wt.%V_2O_5 catalysts. This suggests a mechanism not involving the W or Mo species. However, formaldehyde presence slightly inhibits the standard SCR reaction and also leads to high CO emissions.

Overall, the replacement of WO_3 with MoO_3 in V-based SCR catalysts leads to slightly lower CO emissions during standard SCR in the presence of propylene or dodecane, an aspect that is critical for such catalysts. However, due to the decrease of the specific surface area an inferior SCR activity was measured for the MoO_3-containing catalysts at low temperatures. Hence, for a final assessment, the improvement of the structural stability of Mo-promoted catalysts, including the addition of Mo species to the V-WTi catalyst or more advanced catalyst formulations, represents the next step in obtaining efficient SCR on DPF exhaust gas aftertreatment systems.

Acknowledgments

The authors gratefully acknowledge financial support of this work via provision of a PhD scholarship to L. Zheng by China Scholarship Council (CSC). We thank Dr. D. Doronkin, D. Zengel and J. Pesek for technical support with respect to catalysts preparation and testing, A. Beilmann for the BET measurements. We gratefully acknowledge KIT and Deutsche Forschungsgemeinschaft (DFG) for financing the Renishaw inVia Reflex Spectrometer System (INST 121384/73-1).

References

1. Deutschmann O, Grunwaldt J-D (2013) Exhaust Gas Aftertreatment in Mobile Systems: Status, Challenges, and Perspectives. Chem Ing Tech 85 (5):595-617
2. Twigg MV (2011) Catalytic control of emissions from cars. Catal Today 163 (1):33-41
3. Busca G, Lietti L, Ramis G, Berti F (1998) Chemical and Mechanistic Aspects of the Selective Catalytic Reduction of NO_x by Ammonia over Oxide Catalysts: A Review. Appl Catal B 18 (1):1-36

4. Gao F, Kwak JH, Szanyi J, Peden CHF (2013) Current Understanding of Cu-Exchanged Chabazite Molecular Sieves for Use as Commercial Diesel Engine DeNO(x) Catalysts. Top Catal 56 (15-17):1441-1459
5. Ruggeri M, Nova I, Tronconi E (2013) Experimental Study of the NO Oxidation to NO_2 Over Metal Promoted Zeolites Aimed at the Identification of the Standard SCR Rate Determining Step. Top Catal 56 (1-8):109-113
6. He YY, Ford ME, Zhu MH, Liu QC, Tumuluri U, Wu ZL, Wachs IE (2016) Influence of catalyst synthesis method on selective catalytic reduction (SCR) of NO by NH_3 with V_2O_5-WO_3/TiO_2 catalysts. Appl Catal B 193:141-150
7. Marberger A, Elsener M, Ferri D, Kröcher O (2015) VOx Surface Coverage Optimization of V_2O_5/WO_3-TiO_2 SCR Catalysts by Variation of the V Loading and by Aging. Catalysts 5 (4):1704-1720
8. Ottinger N, Veele R, Xi Y, Liu ZG (2016) Conversion of Short-Chain Alkanes by Vanadium-Based and Cu/Zeolite SCR Catalysts. SAE International J Engines 9 (2):1241-1246
9. Wagner DV, Yang Z. China V gasoline and diesel fuel quality standards, 2014 (available at https://wwwtheicctorg/publications/china-v-gasoline-and-diesel-fuel-quality-standards). Accessed on 21.06.2018.
10. Forzatti P (2001) Present status and perspectives in de-NOx SCR catalysis. Appl Catal 222 (1-2):221-236
11. Murkute AD, Vanderwiel D (2015) Active Sites Evaluation of Vanadia Based Powdered and Extruded SCR Catalysts Prepared on Commercial Titania. Catal Lett 145 (6):1224-1236
12. Tronconi E, Nova I, Ciardelli C, Chatterjee D, Weibel M (2007) Redox features in the catalytic mechanism of the "standard" and "fast" NH_3-SCR of NO_x over a V-based catalyst investigated by dynamic methods. J Catal 245 (1):1-10
13. Lietti L, Nova I, Ramis G, Dall'Acqua L, Busca G, Giamello E, Forzatti P, Bregani F (1999) Characterization and Reactivity of V_2O_5-MoO_3/TiO_2 De-NOx SCR Catalysts. J Catal 187 (2):419-435
14. Liu S, Obuchi A, Oi-Uchisawa J, Nanba T, Kushiyama S (2001) Synergistic catalysis of carbon black oxidation by Pt with MoO_3 or V_2O_5. Appl Catal B 30 (3):259-265
15. Tan J, Solbrig C, Schmieg SJ (2011) The Development of Advanced 2-Way SCR/DPF Systems to Meet Future Heavy-Duty Diesel Emissions. SAE Tech Paper No. 2011-01-1140
16. Johansen K, Bentzer H, Kustov A, Larsen K, Janssens TVW, Barfod RG (2014) Integration of Vanadium and Zeolite Type SCR Functionality into DPF in Exhaust Aftertreatment Systems - Advantages and Challenges. SAE Tech Paper No. 2014-01-1523
17. López - De Jesús YM, Chigada PI, Watling TC, Arulraj K, Thorén A, Greenham N, Markatou P (2016) NO_x and PM Reduction from Diesel Exhaust Using Vanadia SCRF®. SAE Int J Engines 9 (2):1247-1257
18. Bertole C (2018) Formaldehyde Oxidation over Emission Control Catalysts. SAE Tech Paper No. 2018-01-1274
19. Andersson J, Antonsson M, Eurenius L, Olsson E, Skoglundh M (2007) Deactivation of diesel oxidation catalysts: Vehicle- and synthetic aging correlations. Appl Catal B 72 (1):71-81
20. Ganesh D, Nagarajan G, Mohamed Ibrahim M (2008) Study of performance, combustion and emission characteristics of diesel homogeneous charge compression ignition (HCCI) combustion with external mixture formation. Fuel 87 (17):3497-3503
21. Bauer M, Wachtmeister G (2009) Formation of formaldehyde in lean-burn gas engines. MTZ 70 (7-8):50-57
22. Finocchio E, Baldi M, Busca G, Pistarino C, Romezzano G, Bregani F, Toledo GP (2000) A study of the abatement of VOC over V_2O_5-WO_3-TiO_2 and alternative SCR catalysts. Catal Today 59 (3):261-268
23. Koebel M, Elsener M (1998) Oxidation of diesel-generated volatile organic compounds in the selective catalytic reduction process. Ind Eng Chem Res 37 (10):3864-3868
24. Busca G, Baldi M, Pistarino C, Gallardo Amores JM, Sanchez Escribano V, Finocchio E, Romezzano G, Bregani F, Toledo GP (1999) Evaluation of V_2O_5-WO_3-TiO_2 and alternative SCR catalysts in the abatement of VOCs. Catal Today 53 (4):525-533
25. Christensen JM, Grunwaldt J-D, Jensen AD (2016) Importance of the oxygen bond strength for catalytic activity in soot oxidation. Appl Catal B 188:235-244
26. Watling TC, Lopez Y, Pless JD, Sukumar B, Klink W, Markatou P (2013) Removal of Hydrocarbons and Particulate Matter Using a Vanadia Selective Catalytic Reduction Catalyst: An Experimental and Modeling Study. SAE Int J Engines 6 (2):882-897
27. Ottinger NA, Xi, Y., Foley, B., Mnichowicz, B., Liu, Z. (2013) Hydrocarbon Interaction with Vanadium-based SCR Catalysts-A Mechanistic Study. Proc CLEERS Workshop
28. Heo I, Lee Y, Nam I-S, Choung JW, Lee J-H, Kim H-J (2011) Effect of hydrocarbon slip on NO removal activity of CuZSM5, FeZSM5 and V_2O_5/TiO_2 catalysts by NH_3. Microporous Mesoporous Mater 141 (1):8-15
29. Japke E, Casapu M, Trouillet V, Deutschmann O, Grunwaldt J-D (2015) Soot and hydrocarbon oxidation over vanadia-based SCR catalysts. Catal Today 258:461-469
30. Leocadio ICL, Braun S, Schmal M (2004) Diesel soot combustion on Mo/Al_2O_3 and V/Al_2O_3 catalysts: investigation of the active catalytic species. J Catal 223 (1):114-121

31. Debecker DP, Delaigle R, Bouchmella K, Eloy P, Gaigneaux EM, Mutin PH (2010) Total oxidation of benzene and chlorobenzene with MoO_3- and WO_3-promoted V_2O_5/TiO_2 catalysts prepared by a nonhydrolytic sol-gel route. Catal Today 157 (1):125-130
32. Mei C, Yuan Y, Li X, Mei D (2016) Microscopic Phase Structure of Mo-based Catalyst and Its Catalytic Activity for Soot Oxidation. Bull Chem React Eng Catal:9
33. Mei C, Mei D, Yue S, Chen Z, Yuan Y (2017) Optimized Heating Rate and Soot-catalyst Ratio for Soot Oxidation over MoO3 Catalyst. Bull Chem React Eng Catal:7
34. Toniolo FS, Barbosa-Coutinho E, Schwaab M, Leocadio ICL, Aderne RS, Schmal M, Pinto JC (2008) Kinetics of the catalytic combustion of diesel soot with MoO_3/Al_2O_3 catalyst from thermogravimetric analyses. Appl Catal A 342 (1):87-92
35. Parus W, Paterkowski W (2009) Catalytic oxidation of organic pollutants. Pol J Chem Technol 11 (4):30-37
36. Bertinchamps F, Grégoire C, Gaigneaux EM (2006) Systematic investigation of supported transition metal oxide based formulations for the catalytic oxidative elimination of (chloro)-aromatics: Part II: Influence of the nature and addition protocol of secondary phases to VO_x/TiO_2. Appl Catal B 66 (1):10-22
37. Alemany LJ, Lietti L, Ferlazzo N, Forzatti P, Busca G, Giamello E, Bregani F (1995) Reactivity and Physicochemical Characterization of V_2O_5-WO_3/TiO_2 De-NOx Catalysts. J Catal 155 (1):117-130
38. Bond GC, Tahir SF (1991) Vanadium oxide monolayer catalysts Preparation, characterization and catalytic activity. Appl Catal 71 (1):1-31
39. Vermaire DC, van Berge PC (1989) The preparation of WO_3/TiO_2 and WO_3/Al_2O_3 and characterization by temperature-programmed reduction. J Catal 116 (2):309-317
40. Kompio P, Brückner A, Hipler F, Auer G, Loffler E, Grünert W (2012) A new view on the relations between tungsten and vanadium in V_2O_5-WO_3/TiO_2 catalysts for the selective reduction of NO with NH_3. J Catal 286:237-247
41. Srnak T, Dumesic J, Clausen B, Törnqvist E, Topsøe N-Y (1992) Temperature-programmed desorption/reaction and in situ spectroscopic studies of vanadia/titania for catalytic reduction of nitric oxide. J Catal 135 (1):246-262
42. Michalow-Mauke KA, Lu Y, Ferri D, Graule T, Kowalski K, Elsener M, Kröcher O (2015) $WO_3/CeO_2/TiO_2$ Catalysts for Selective Catalytic Reduction of NO_x by NH_3: Effect of the Synthesis Method. CHIMIA Int J Chem 69 (4):220-224
43. Song I, Youn S, Lee H, Lee SG, Cho SJ, Kim DH (2017) Effects of microporous TiO_2 support on the catalytic and structural properties of V_2O_5/microporous TiO_2 for the selective catalytic reduction of NO by NH_3. Appl Catal B 210:421-431
44. Balachandran U, Eror NG (1982) Raman-Spectra of Titanium-Dioxide. J Solid State Chem 42 (3):276-282
45. Frank O, Zukalova M, Laskova B, Kurti J, Koltai J, Kavan L (2012) Raman spectra of titanium dioxide (anatase, rutile) with identified oxygen isotopes (16,17,18). Phys Chem Chem Phys 14 (42):14567-14572
46. Ross-Medgaarden EI, Wachs IE (2007) Structural determination of bulk and surface tungsten oxides with UV-vis diffuse reflectance spectroscopy and Raman spectroscopy. J Phys Chem C 111 (41):15089-15099
47. Went GT, Oyama ST, Bell AT (1990) Laser Raman-Spectroscopy of Supported Vanadium-Oxide Catalysts. J Phys Chem 94 (10):4240-4246
48. Reiche MA, Ortelli E, Baiker A (1999) Vanadia grafted on TiO_2-SiO_2, TiO_2 and SiO_2 aerogels - Structural properties and catalytic behaviour in selective reduction of NO by NH_3. Appl Catal B 23 (2-3):187-203
49. Roark RD, Kohler SD, Ekerdt JG, Kim DS, Wachs IE (1992) Monolayer Dispersion of Molybdenum on Silica. Catal Lett 16 (1-2):77-83
50. Rasmussen SB, Mikolajska E, Daturi M, Bañares MA (2012) Structural characteristics of an amorphous VPO monolayer on alumina for propane ammoxidation. Catal Today 192 (1):96-103
51. Zhao C, Wachs IE (2008) Selective oxidation of propylene over model supported V_2O_5 catalysts: Influence of surface vanadia coverage and oxide support. J Catal 257 (1):181-189
52. Topsøe NY, Dumesic JA, Topsøe H (1995) Vanadia-Titania Catalysts for Selective Catalytic Reduction of Nitric-Oxide by Ammonia: I.I. Studies of Active Sites and Formulation of Catalytic Cycles. J Catal 151 (1):241-252
53. Tronconi E, Nova I, Ciardelli C, Chatterjee D, Weibel M (2007) Redox features in the catalytic mechanism of the "standard" and "fast" NH_3-SCR of NO_x over a V-based catalyst investigated by dynamic methods. J Catal 245 (1):1-10
54. Bertinchamps F, Treinen M, Eloy P, Dos Santos AM, Mestdagh MM, Gaigneaux EM (2007) Understanding the activation mechanism induced by NO_x on the performances of VO_x/TiO_2 based catalysts in the total oxidation of chlorinated VOCs. Appl Catal B 70 (1):360-369